

# Low cross-talk polarization splitter based on photonic crystal waveguide with tunable air hole arrays

CANCAN WANG, HAO GUO, XIONG ZHANG\*, YIPING CUI

*Advanced Photonics Center, School of Electronic Science and Engineering, Southeast University, Nanjing 210096, P. R. China*

We proposed and numerically investigated a novel two-dimensional (2D) photonic crystal (PhC)-based polarization splitter. It was demonstrated that by introducing single air hole defect into the PhC structure, a low cross-talk polarization splitter can be realized with significantly minimized reflection occurring at the interface between the dielectric material and air. For an operating wavelength of 1.55  $\mu\text{m}$ , an extinction ratio higher than 15 dB has been achieved in this study. The low cross-talk feature together with the high tolerance of the variation in the size of the air hole arrays make the device proposed suitable for the integrated optical circuits.

(Received November 1, 2012; accepted April 11, 2013)

*Keywords:* Polarization-splitter, Photonic crystal, Light extinction ratio

## 1. Introduction

The periodically varied index of refraction in photonic crystal (PhC) structure may be utilized to forbid light propagation in certain wavelength ranges, generating the so-called photonic band gaps (PBG) [1, 2]. Within the PBG, no lights with any modes are allowed to propagate in the PhC and the density of states is zero. By introducing linear defects into the PhC, however, the light transmission path can be modulated. Similar to the impurity-induced energy levels in semiconductors, the defect-related modes will be created within the PBG if the irregular regions like the linear defect are introduced into the perfect PhC structure. As a result, the light that propagates along the waveguide with a frequency within the PBG will be confined to the linear defect, and to propagate along the defect.

Many compact photonic crystal waveguide devices, such as optical polarization splitters [3], power splitters [4], flat lens [5,6], and optical demultiplexers [7, 8], have been investigated to date. Among them, the polarization splitter is one of the key functional components in the photonic integrated circuits and the optical communication systems [9, 10]. The PhC polarization splitters based on directional coupler [11], self-collimation [12], and negative/positive refraction effect [13] have been studied recently. However, since the polarization splitter based on the directional couplers has a small separating angle for TE and TM polarized lights, bent waveguides have to be introduced to realize a large separation angle. Employing positive refraction for one polarization mode and negative refraction for another mode may be an effective method in separating the two polarization modes. This, however, inevitably results in significant increase in the device size and the energy

lose.

The PhC polarization splitter based on the polarization-dependent dispersion properties [14] is of a compact device size and potentiality for integrating with other PhC devices. However, some problems have to be solved before it can be used in the integrated photonic circuits. In this paper we proposed and investigated a novel type of polarization-dependent splitter with an extinction ratio higher than 15 dB and extremely low cross-talk feature by means of plane wave expansion (PWE) method. Our device is based on a two-dimensional photonic crystal structure consisting of a triangular lattice of air holes in dielectric material, which was demonstrated to be very powerful in separating the light waves with different polarizations.

## 2. Modeling and theory

We consider a triangular lattice of air holes made on Ge substrate that has a dielectric constant of  $\epsilon = 18.5$ . The ratio between the air hole radius and the lattice constant is  $r/a = 0.49$ . Fig. 1 shows the proposed polarization splitter consisting of three linear waveguides: one input waveguide which is formed by removing an entire row of air holes as indicated by Ch1 in Fig. 1; one straight output waveguide as indicated by Ch2 in Fig. 1; and one oblique output waveguide connected to the input waveguide with an angle of  $60^\circ$  as indicated by Ch3 in Fig. 1. Both of the two output waveguides are composed of the air holes with reduced radius, as shown in Fig. 1.

The band structures and the dispersion curves of the PhC waveguides are calculated with the PWE method. The PWE method is used for theoretical analysis of

photonic crystal structures in terms of superposition of a set of plane waves. According to our calculated results, the PBG located in between the normalized frequency  $a/\lambda$  of 0.418–0.514, within which neither TE nor TM mode light can propagate in the PhC waveguides.

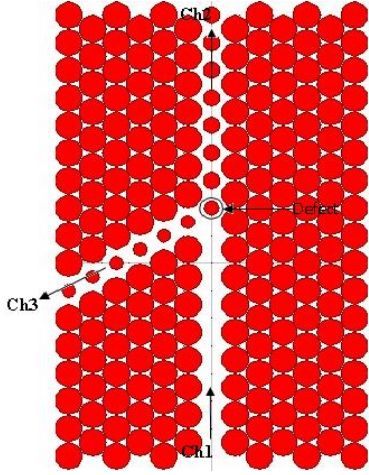


Fig. 1. Schematic structure of the proposed polarization splitter made of a two-dimensional photonic crystal with a triangular lattice of air holes in dielectric material, Ge.

Nevertheless, the propagation of the guided lights can be modified by altering the size of air holes along a single row of the output PhC waveguide. Furthermore, since the dispersion properties of the guided lights are different for TE and TM polarized lights, we can make use of this feature to modify the propagation properties of the guided lights with different modes. For certain sizes of the air holes in the output waveguide, only the guided TM polarization modes within a special frequency range are allowed to propagate due to the existence of PBG for TE polarization modes. The dispersion property for the guided lights in Ch2 is shown in Fig. 2. It is clear that there are only TM modes in the PBG (indicated by grey areas) localized in the region of  $0.423 < a/\lambda < 0.445$  as the radius of the air holes in the waveguide is set to  $0.291a$ . In other words, the TM polarized lights are allowed to propagate within this frequency range whereas the TE polarized lights are prohibited to propagate in the waveguide Ch2 due to the PBG effect.

On the other hand, the TE mode lights incident along Ch1 can be collected and guided into a closely placed waveguide Ch3 with certain size of air hole in a row right next to the entrance of waveguide Ch2. Namely, within the operating frequency range of 0.423–0.445 ( $a/\lambda$ ), the incident TM mode lights propagate from Ch1 to Ch2 while the incident TE mode lights propagate from Ch1 to Ch3 so that the TM and TE mode lights are spatially separated (split). Moreover, it was found that the performance of the polarization splitter is nearly independent of the size of the air hole in the oblique output waveguide. In fact, our calculation results indicate

that there is only approximately 3% deviation in the PBG for the wavelength range interested even if the air hole radius varies from  $0.23a$  to  $0.26a$  or increases by 13%. This high tolerance of our device is of particular importance in the fabrication of the photonic crystal integrated circuits.

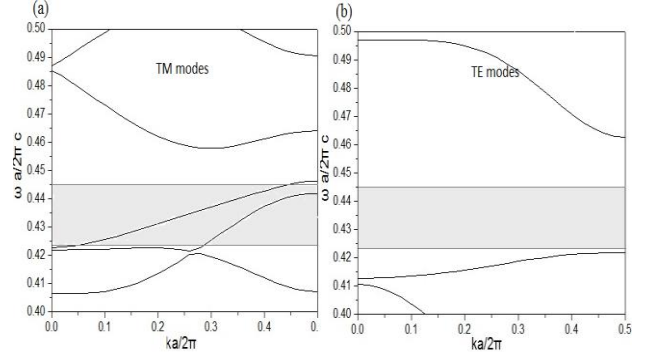


Fig. 2. Dispersion properties for the guided TM (a) and TE (b) polarization modes along Ch2. The gray areas illustrate the PBG in the normalized frequency range of 0.423–0.445 within which there are only TM modes.

### 3. Results and discussion

For simplicity, it was assumed that a Gaussian light wave at normalized frequency  $a/\lambda = 0.435$  was input into the waveguide Ch1. The PhC lattice constant  $a$  was selected to be  $0.674 \mu\text{m}$  and the operating wavelength was  $1.55 \mu\text{m}$ . The calculated steady-state electromagnetic field distribution patterns for both TM and TE polarized lights with the same frequency are shown in Fig. 3.

The simulation is based on the well-known finite-difference time domain (FDTD) technique. The FDTD method [15] was utilized to calculate the light transmission characteristics for the polarization splitter with perfectly matched layers (PMLs) absorbing boundary conditions [16]. For a linear isotropic material in a source-free region, the time-dependent Maxwell's equations can be written as below:

$$\nabla \times \vec{E} = -\mu(r) \frac{\partial \vec{H}}{\partial t} \quad (1)$$

$$\nabla \times \vec{H} = \varepsilon(r) \frac{\partial \vec{E}}{\partial t} + \sigma(r) \vec{E} \quad (2)$$

Where,  $\varepsilon(r)$ ,  $\mu(r)$ , and  $\sigma(r)$  are the position dependent permittivity, permeability, and conductivity of the material, respectively. In the 2D case, the field can be decoupled into two transversely polarized modes, the E- and H-polarization modes. These equations can be discretized in terms of space and time by the so-called Yee-cell technique. The following FDTD time stepping

formulas describe spatial and time discretizations of Eq. (1) and (2) on a discrete 2D mesh within the x-y coordinate system for the E-polarization mode,

$$H_x \Big|_{i,j+1/2}^{n+1/2} = H_x \Big|_{i,j+1/2}^{n-1/2} - \frac{\Delta t}{\mu_0} \left( \frac{E_z \Big|_{i,j+1}^n - E_z \Big|_{i,j}^n}{\Delta y} \right) \quad (3)$$

$$H_y \Big|_{i+1/2,j}^{n+1/2} = H_y \Big|_{i+1/2,j}^{n-1/2} + \frac{\Delta t}{\mu_0} \left( \frac{E_z \Big|_{i+1,j}^n - E_z \Big|_{i,j}^n}{\Delta x} \right) \quad (4)$$

$$E_z \Big|_{i,j}^{n+1} = E_z \Big|_{i,j}^n + \frac{\Delta t}{\epsilon_{i,j}} \left( \frac{H_y \Big|_{i+1/2,j}^{n+1/2} - H_y \Big|_{i-1/2,j}^{n+1/2}}{\Delta x} - \frac{H_x \Big|_{i,j+1/2}^{n+1/2} - H_x \Big|_{i,j-1/2}^{n+1/2}}{\Delta y} \right) \quad (5)$$

where the index  $n$  denotes the discrete time step, indices  $i$  and  $j$  denote the discretized grid points in the x-y planes, respectively.

If the following condition is satisfied, FDTD time-stepping formulas are numerically stable:

$$\Delta t \leq \frac{1}{c \sqrt{\frac{1}{\Delta x^2} + \frac{1}{\Delta y^2}}} \quad (6)$$

where  $c$  is the speed of light in free space.

The perfectly match layers (PMLs) are utilized to truncate the computational region and to avoid the reflections from the outer boundary. The two dimensional FDTD method is used to analyze the spectral characteristics of the structure in this study.

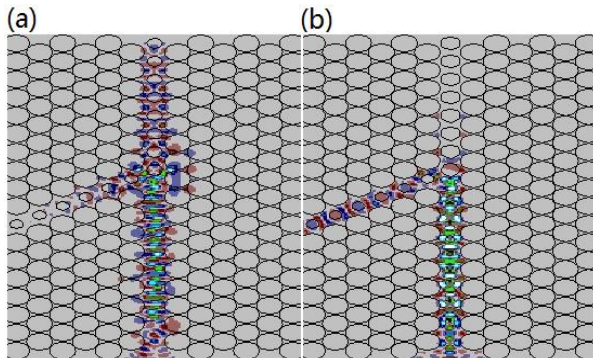


Fig. 3. The calculated steady-state electromagnetic field distribution for TM (a) and TE (b) polarized lights.

From Fig. 3, it can be seen that the outgoing light beams with the TM and TE polarization modes are split quite well with a separating angle of approximately  $120^\circ$ . However, for the TM (TE) mode, there is a little amount of undesirable power leakage into the waveguide Ch3 (Ch2) although the leaked light power degrades nearly completely in a short distance from the intersection of the waveguides, Ch1, Ch2, and Ch3. We speculate that this kind of light power leakage was resulted by the reflection occurring at the 2D photonic crystal–air interface due to the large difference in refractive index between air and the 2D photonic crystal. In order to reduce the light power leakage or modify the far field distribution pattern, a single hole defect with a radius of  $R_M$  was introduced at the intersection of the waveguides, Ch1, Ch2, and Ch3,

indicated by a circle in Fig. 1.

Fig. 4 shows the electromagnetic field distribution patterns for both TM (a) and TE (b) polarized lights in the case where the radius of the single hole defect is  $R_M = 0.27a$  at the normalized frequency of  $a/\lambda = 0.435$ . As demonstrated clearly in Fig. 4, the power leakage for both TM and TE polarized lights was greatly suppressed, implying that the performance of the polarization splitter with a single hole defect has been significantly improved. It is expected that the device performance may be further enhanced by optimizing the size of the introduced single hole defect.

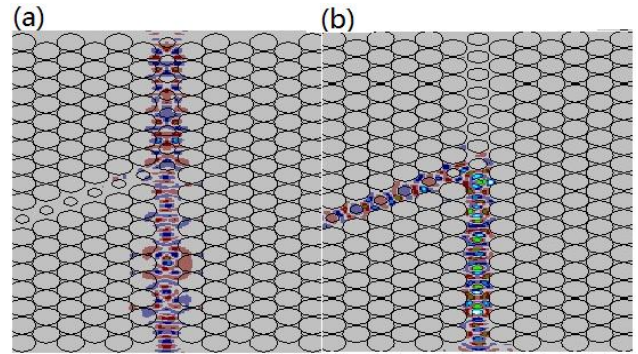


Fig. 4. The steady-state electromagnetic field distribution for TM (a) and TE (b) polarized lights with the optimized polarization splitter where a single hole defect with a radius of  $R_M = 0.27a$  was introduced at the intersection of the waveguides Ch1, Ch2, and Ch3 as shown in Fig. 1.

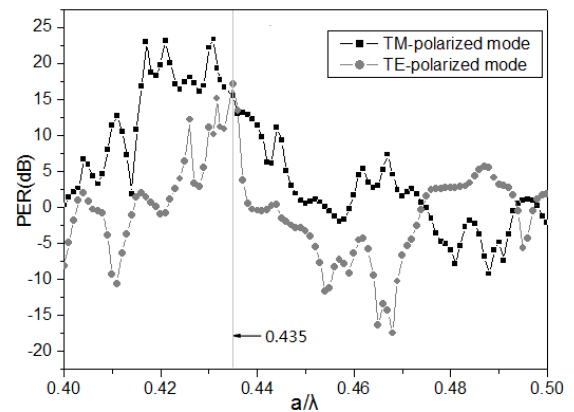


Fig. 5. The extinction ratios for both TM and TE incident light modes as a function of the normalized frequency.

One of the most important parameters for the polarization splitter is the extinction ratio for the incident light as a function of the normalized frequency. The extinction ratios were calculated in terms of the expression  $dB = 10 \log_{10} P_{p1} / P_{p2}$ , where  $P_{p1}$  and  $P_{p2}$  are the light powers for the primary and transverse polarizations at the same port, respectively. For an optical communication system, the extinction ratios

determine the level of the noise disturbance induced from any unwanted polarization mode lights transmitting through a particular output waveguide. As shown in Fig. 5, for instance, the extinction ratios for the TM- and TE-polarized light modes at the normalized frequency of  $a/\lambda = 0.435$  (indicated by the vertical gray line) are 15.6 dB and 17.1 dB, respectively. These high extinction ratios are another advantage of the proposed polarization splitter with air hole defect over the conventional counterparts without any point defects.

#### 4. Conclusions

In this paper, we have presented the numerical design and analysis of the polarization splitter based on 2D-photonic crystal waveguide. An extremely low cross-talk as well as an extinction ratio higher than 15 dB have been achieved with the proposed polarization splitter within which there is a specially designed single air hole defect introduced at the intersection of the three waveguides. For an operating wavelength of 1.55  $\mu\text{m}$ , the proposed polarization splitter was demonstrated to be very powerful in separating the TE- and TM-polarized lights with a large angle. Besides the low cross-talk feature, due to the low sensitivity of the photonic band gap on the variation in the air hole arrays, high tolerance of the device is expected, which is crucial in the fabrication of the photonic crystal integrated circuits.

#### Acknowledgements

The authors would like to thank Mr. Hongjun Chen for his fruitful discussion throughout this work.

#### References

- [1] E. Yablonovitch, *Phys. Rev. Lett.* **58**, 2059 (1987).
- [2] S. John, *Phys. Rev. Lett.* **58**, 2486 (1987).
- [3] S. Liu, S. G. Li, Y. Du, *Opt. Laser Technol.* **44**, 1813 (2012).
- [4] T. B. Yu, L. J. He, X. H. Deng, L. G. Fang, N. H. Liu, *Opt. Engineering* **50**, 114601 (2011).
- [5] J. J. Liu, Z. G. Fan, H. L. Hu, M. H. Yang, C. Y. Guan, L. B. Yuan, H. Guo, X. Zhang, *Opt. Lett.* **37**, 1730 (2012).
- [6] J. J. Liu, B. J. Zuo, S. Q. Chen, H. L. Hu, H. S. Xiao, W. Zhang, Z. G. Fan, H. Guo, X. Zhang, *Opt. Engineering* **51**, 074005 (2012).
- [7] M. Koshiba, *J. Lightwave Technol.* **19**, 1970 (2001).
- [8] T. Niemi, L. H. Frandsen, K. K. Hede, A. Harpøth, P. I. Borel, M. Kristensen, *IEEE Photon. Technol. Lett.* **18**, 226 (2006).
- [9] T. Hayakawa, S. Asakawa, Y. Kokubun, J. *Lightwave Technol.* **15**, 1165 (1997).
- [10] L. Soldano, A. H. de Vreede, M. K. Smit, B. H. Verbeek, E. G. Metaal, F. H. Groen, *IEEE Photon. Technol. Lett.* **6**, 402 (1994).
- [11] T. B. Yu, M. H. Wang, X. Q. Jiang, Q. H. Liao, J. Y. Yang, *J. Opt. A: Pure Appl. Opt.* **9**, 37 (2007).
- [12] X. Y. Chen, Z. X. Qiang, D. Y. Zhao, *Opt. Commun.* **284**, 490 (2011).
- [13] X. Y. Ao, S. L. He, *Opt. Lett.* **30**, 2152 (2005).
- [14] X. Y. Chen, P. J. Yao, B. Chen, F. Li, J. Y. Zhang, J. P. Xie, H. Ming, S. H. Fan, *Chin. Phys. Lett.* **21**, 1285 (2004).
- [15] A. Taflove, S. C. Hagness, 2nd Ed., Artech House, Boston, Massachusetts (2000).
- [16] J. P. Berenger, *J. Comput. Phys.* **114**, 185 (1994).

\*Corresponding author: xzhang62@yahoo.cn